JOURNAL OF MATERIALS SCIENCE **39** (2004) 4841–4847

The effect of prestrain on the natural aging and fracture behaviour of AA6111 aluminum

G. K. QUAINOO*, S. YANNACOPOULOS†
Department of Mechanical Engineering, 57 Campus Drive, University of Saskatchewan, Saskatoon, SK, S7N 5A9
E-mail: spiro@engr.usask.ca

In this paper, the effect of prestrain on the T4 behaviour as well as fracture behaviour of AA6111 has been investigated with a view to understanding its strengthening characteristics under this condition. The evaluation methods include tensile testing, differential scanning calorimetry (DSC) and fractography using scanning electron microscopy (SEM). It was found that AA6111 develops increased strength with increasing levels of prestrain during natural aging. The application of plastic prestrain prior to natural aging increases the speed with which the various phases form during natural aging, while decreasing the volume fraction of GPI zones. Prior prestrain and subsequent natural aging show improvement in the dimpled tensile fracture. However, the role of intermetallic particles is significant in that they serve as nucleation sites for fracture.

1. Introduction

In the continuing drive for weight reduction in new automobile designs, the 6000 series Al-Mg-Si alloys have emerged as the most promising age-hardenable body sheet material in the automotive industry. Currently, in North America, the predominant candidate sheet alloy used is the AA6111, an Al-Mg-Si-Cu alloy. This alloy has good combination of strength and formability in the T4 temper. Its strength can be further enhanced by precipitation hardening during the final paint bake process in the automotive manufacturing process.

The effect of precipitation on the strength of various Al-Mg-Si alloys has been investigated and reported very extensively in the open literature, for example [1–6], their strength being attributed to the precipitation of the Mg_2Si phase during artificial aging. It is noted that in all these investigations, only the strength increase due to precipitation mostly has been considered.

In recent times however, a number of researchers have made some attempts at investigating the effect of natural aging as well as preaging on precipitation in Al-Mg-Si alloys. For example Poole and co-workers [7] investigated the effect of natural aging on the evolution of yield strength during artificial aging for Al-Mg-Si-(Cu) alloys. They observed that with long term natural aging prior to artificial aging, the initial component of yield stress (arising from natural aging) gradually decreased as aging progressed. It is also very established that the presence of Cu in Al-Mg-Si alloys enhances the precipitation kinetics of these alloys [8–13]. Murayama *et al.* [14] and Murayama and Hono [15] using the 3 dimensional atom probe field ion microscopy (APFIM) technique have investigated the adverse age-hardening effect due to natural aging on precipitation in Al-Mg-Si alloys. They found that separate Mg- and Si-clusters are present in the as-quenched condition, but Mg and Si atoms aggregate during natural aging to form Mg-Si co-clusters. It is envisaged that the involvement of Cu-containing clusters during natural aging will alter the precipitation sequence in Al-Mg-Si-Cu alloys and therefore affect the natural aging behaviour of these alloys.

Although it is generally believed that long term natural aging would improve the strengthening characteristics of AA6111 alloys, to the best of our knowledge not much has been reported in the open literature, let alone the effect of prestrain on the natural aging behaviour of this alloy. In the present investigation, the effect of prestrain on the natural aging behaviour of AA6111 aluminum is studied with a view to understanding its contribution to the age-hardening characteristics of this alloy under this condition. This is very crucial since in the present and future applications of this alloy for external and internal automobile body panels, the interaction between prestrain and natural aging becomes paramount in the manufacturing process. Again, the forming of various parts of an automobile body panel will involve the application of various levels of prestrain, which will turn to influence the aging characteristics of the alloy. Furthermore, natural aging is unavoidable in the automobile manufacturing processing line. The evaluation methods employed

*On Study Leave from: Physics Department, University of Cape Coast, Cape Coast, Ghana.
†Author to whom all correspondence should be addressed.

TABLE I Chemical composition limit of AA6111 (weight percent)

	Cu	Fe	Mg	Mn	Si	Ti
Maximum	0.9	0.4	1.0	0.45	1.1	0.10
Minimum	0.5		0.5	0.1	0.6	

in the present study include tensile testing, differential scanning calorimetry (DSC) and scanning electron microscopy (SEM).

2. Experimental procedure

The AA6111 material used in the present study was supplied by Alcan International Limited, Kingston, Ontario, its composition limit is presented in Table I. The material was manufactured by a special technique, the details of which are reported in [16].

2.1. Tensile testing

The tensile specimens were machined from a 1 mm thick stock plate in accordance with ASTM E-8 specifications, with a gauge length of 50 and 12 mm gauge width. They were solution heat treated at $560 \pm 5^{\circ}$C for 30 min in a constant temperature air furnace and cold water quenched. Plastic prestrains of 0, 2, 5 and 10% (by stretching) respectively were then applied to the samples which were subsequently aged at room temperature for various lengths of time. To ensure that the samples did not begin aging between solution heat treatment and tensile testing, they were stored at -10°C. The period between solution heat treatment and prestrain maintained at six to twelve hours to ensure that the material did not begin to naturally age. Tensile tests were then performed on the samples at room temperature using an Instron^{TM} screw-driven machine (model # 1122) at an initial strain rate of 0.025 s^{-1}. The tensile strength and the 0.2% off set yield strength values were determined from the resulting stress vs. strain plot. The percentage elongation was also determined.

2.2. Differential scanning calorimetry (DSC)

DSC analyses of samples subjected to various levels of prestrain (0, 2, 5 and 10%) and naturally aged for various lengths of time were carried out using a temperature-modulated DSC 2910 system (MDSC^{TM}, TA Instrument Inc., USA) which incorporates a liquid nitrogen cooling accessory and a nitrogen gas DSC cell purge. The instrument was calibrated for enthalpy and temperature using a standard high purity elemental indium and operated in the non-modulated regime. Three DSC runs were conducted for each natural aging time in order to ensure reproducibility. All DSC runs began at 30°C and ended at 240°C at a constant heating rate of 10°C min^{-1}. This temperature range was intentionally chosen to isolate GPI zone reactions since they are the most paramount under the natural aging condition. In order to correct for the additional heat flow arising from the difference in weight of the sample pan and the reference pan, and also to compensate for any asymmetry in the measuring system, a preliminary blank experiment was performed with commercially pure aluminum. Thus the heat flow obtained was the difference between the measured and the blank values.

2.3. Scanning electron microscopy (SEM)

The fracture surfaces of AA6111 tensile samples which had been subjected to different levels of prestrain and naturally aged for various lengths of time were examined using a Jeol JSM-5900LV scanning electron microscope (SEM) equipped with INCA energy-dispersion spectrometry (EDS) analysis system.

3. Results and discussion

3.1. Tensile

Figs 1 and 2 show the variation of yield and ultimate tensile strengths with aging time at room temperature respectively, for AA6111 aluminum subjected to

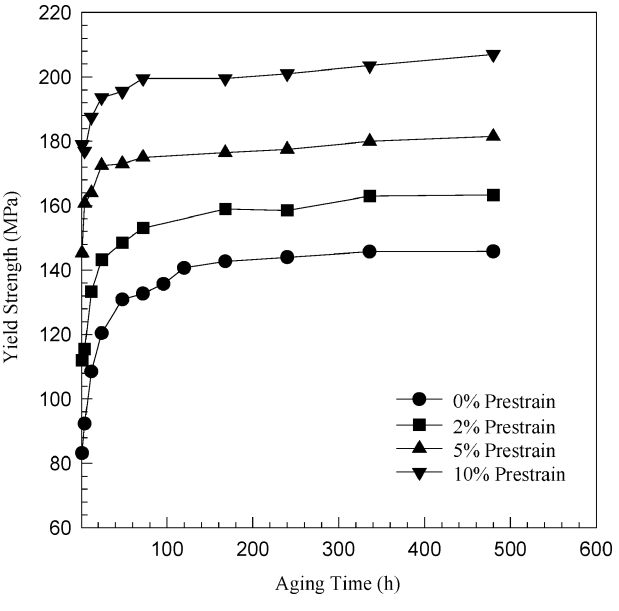

Figure 1 Variation of yield strength with natural aging time for various levels of prestrain in AA6111 aluminum.

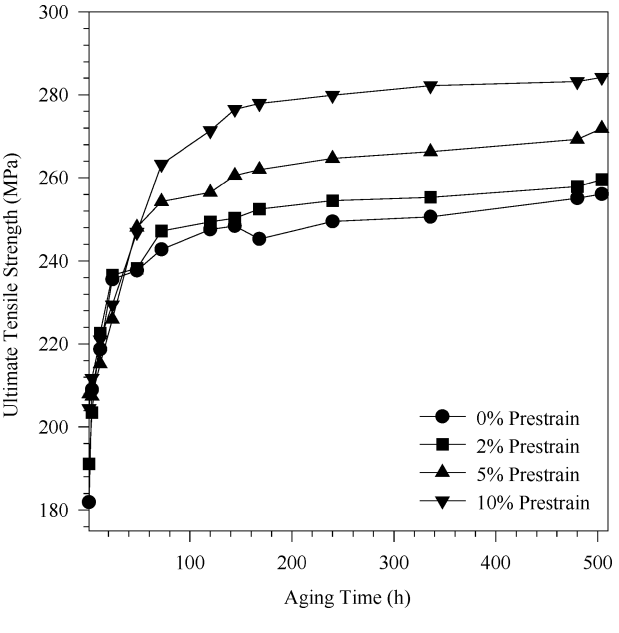

Figure 2 Variation of ultimate tensile strength with natural aging time for various levels of prestrain in AA6111 aluminum.

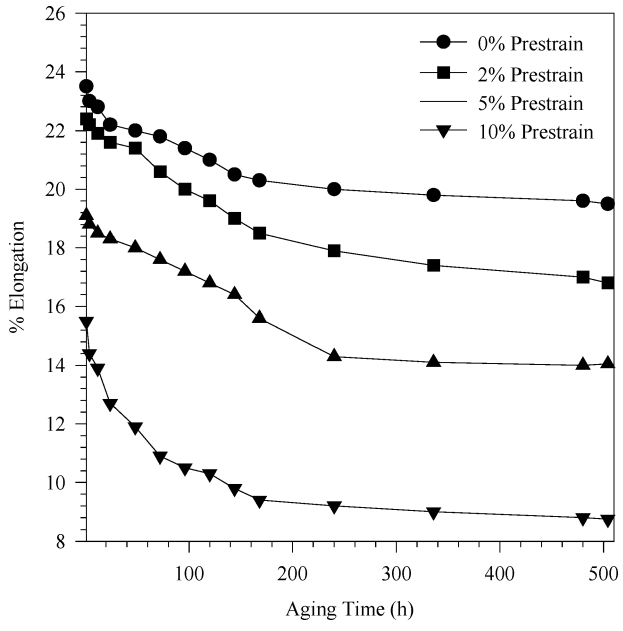

Figure 3 Variation of percentage elongation with natural aging time for various levels of prestrain in AA6111 aluminum.

various levels of prestrain. It can be observed in Fig. 1 that the yield strength rises very sharply within the first 48 h of aging, the sharpness increasing with increasing level of prestrain, after which the rate of increase in yield strength decreases and levels off with further aging. This indicates that the overall aging sequence of AA6111 aluminum is unaffected by the application of plastic prestrain.

However, a few other features of Fig. 1 are worthy of note. First, the unstrained sample attained a monotonic maximum after approximately 120 h of natural aging while the prestrained samples attained a monotonic maximum after about 96 h of natural aging irrespective of the level of prestrain. Thus, the application of plastic prestrain accelerates the early precipitation kinetics of the alloy under the natural aging condition. Secondly, as expected, there is an increase in yield strength with increasing level of prestrain. Fig. 2 also shows general increase of tensile strength with increasing level of prestrain.

Fig. 3 shows the variation of percentage elongation to fracture as a function of natural aging time for various levels of prestrain. There is a continual decrease in percentage elongation to fracture with aging time. A rapid fall in percentage elongation to fracture is observed during aging of up to 48 h, after which the rate of reduction decreases.

The precipitation sequence for Cu-containing Al-Mg-Si alloys for a long time has been traditionally considered to be analogous to the ternary Cu-free Al-Mg-Si alloys shown in Equation 1:

$$\text{SSS} \rightarrow \text{GPI (Mg/Si rich)} \rightarrow \text{GPII (Mg/Si rich)}/\beta'' \rightarrow \beta' \rightarrow \beta \quad (1)$$

However, Gupta and co-workers [17] in their study of the precipitation sequence in AA6111 (an Al-Mg-Si-Cu alloy) proposed another possible sequence that could be

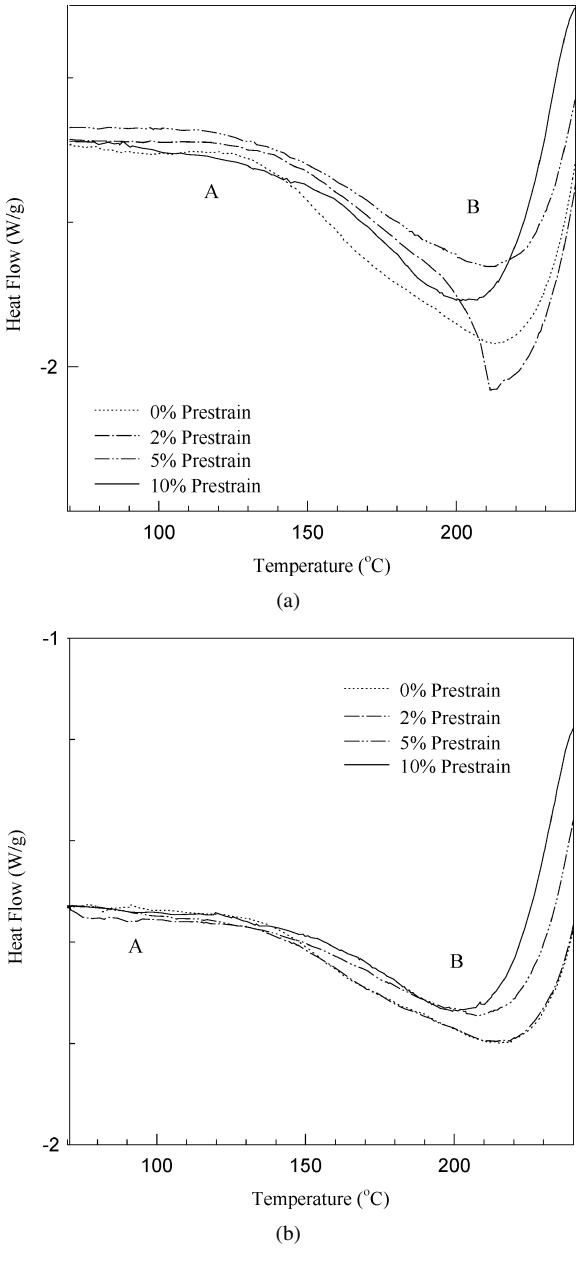

Figure 4 DSC thermograms of quenched samples of AA6111 at various levels of prestrain at: (a) 168 h natural aging and (b) 500 h natural aging.

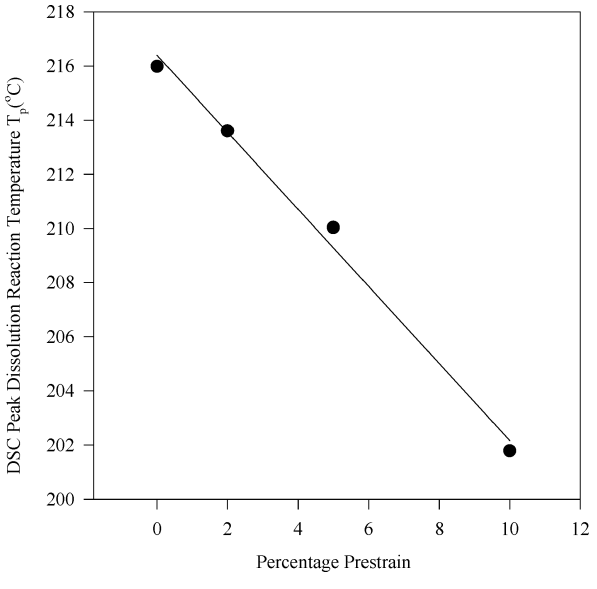

Figure 5 Variation of DSC peak dissolution reaction temperature (T_p) of GPI zones with level of prestrain at 24 h natural aging.

followed as:

$$\text{SSS} \rightarrow \text{GPI (Cu/Al rich)} \rightarrow \text{GPII (Cu/Al rich)}/\theta'' \rightarrow \theta' \rightarrow \theta \quad (2)$$

Recently, the precipitation of the quaternary Q phase and its precursor Q' in Cu-containing Al-Mg-Si has been reported [18–23]. As a result, the precipitation sequence in AA6111 has come to be accepted as:

$$\text{SSS} \rightarrow \text{clusters/GP zones} \rightarrow \beta'' + Q' \rightarrow \text{equilibrium}\, Q + \text{Mg}_2\text{Si} \quad (3)$$

Natural aging is generally believed to be due to the occurrence of clusters of solute atoms followed by the growth of GPI zones. For this particular alloy, this entails the formation of separate Mg-, Si-, Cu-, and co-clusters of Mg-Si and/or Cu-Al [9, 11, 17] in the matrix at the early stages of natural aging (see Equations 1 and 2). These coherent GPI zones distort the aluminum matrix, setting up large strain fields around the GPI zones, which impede the movement of dislocations thereby increasing the strength of the alloy. This stage of precipitation is very complex as the clusters tend to compete with each other, resulting in a lot of dissolution and formation of new clusters. With the formation and growth of the GPI zones, the contribution from increased internal stresses and the movement of quenched in vacancies to the GPI zones gives rise to a further increase in strength. However, further aging increases the size of the GPI zones, resulting in coherency loss, causing the vacancy concentration in the zones and matrix to reach their equilibrium values. Consequently, the rate of increase of strength becomes sluggish as depicted

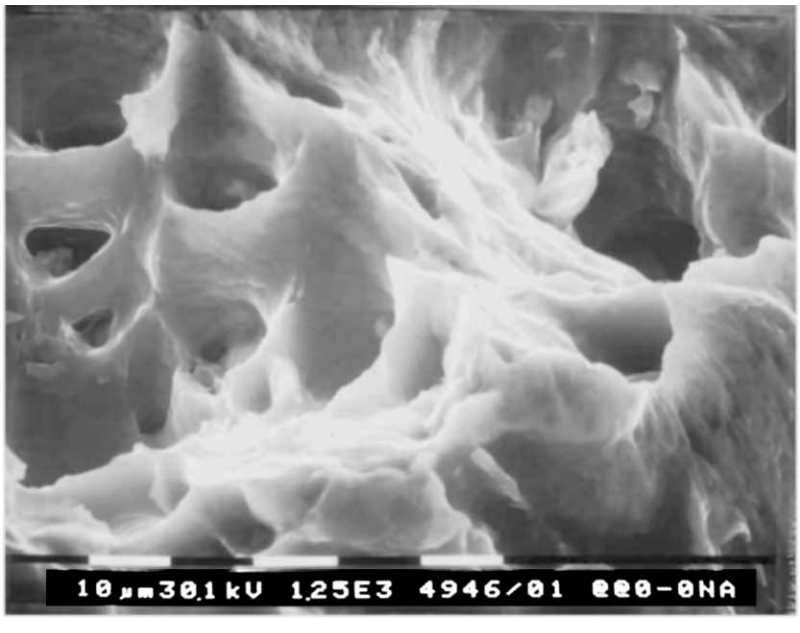

(a)

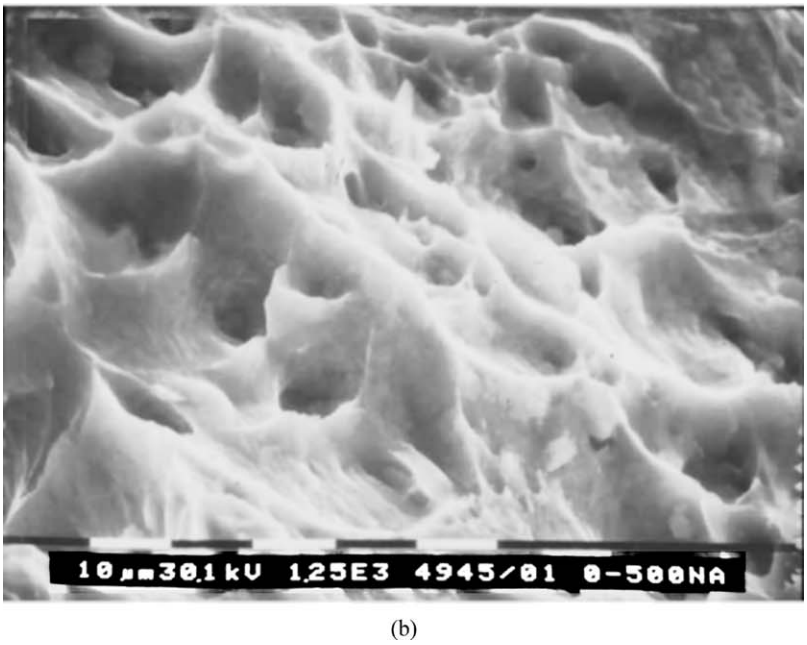

(b)

Figure 6 SEM fractograph of unstrained AA6111 at: (a) 0 h and (b) 500 h natural aging.

by the portion of the curves showing monotonic increase in yield strength with further aging. Furthermore, the application of plastic prestrain to the samples prior to room temperature aging, results in the generation of increased dislocation tangles with increasing level of prestrain and hence an increase in the yield strength of the material. These high energy dislocation sites may favor a faster movement of quenched in vacancies on GPI zones and further increase the yield strength of the material as depicted in Figs 1 and 2.

3.2. Differential scanning calorimetry (DSC)

The DSC thermograms of AA6111 samples, which had been solutionized, quenched, prestrained to various levels and naturally aged for times of 168 and 504 h are shown in Fig. 4a and b. The samples were aged at room temperature for three weeks. The exothermic peak A indicates the formation of GPI zones while the endothermic trough B indicates their dissolution. A visual evaluation of the area under peak A shows that it is larger for the quenched, unstrained and naturally aged sample compared to the quenched, prestrained and naturally aged samples, indicating a decrease in the volume fractions of the GPI zones with increasing level of prestrain. It is further observed that the application of plastic prestrain higher than 2% causes the GPI zone phases to disappear. For the unstrained condition, this may be attributed to the formation of initial clusters of Mg, Si, and/or Cu following quenching and the speed with which these transform into stable GPI zones. This is consistent with the reported results of DSC scans conducted on other Al-Mg-Si alloys [23, 25–29]. It is also

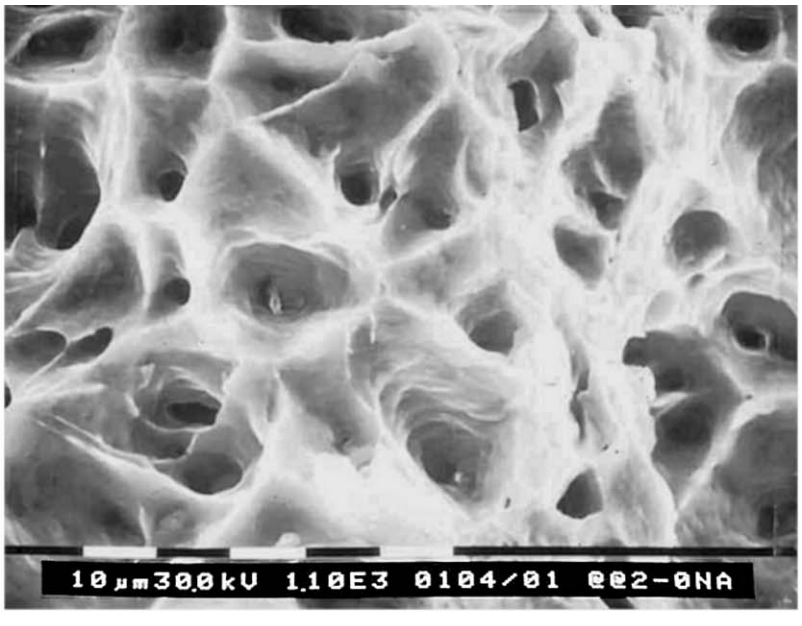

(a)

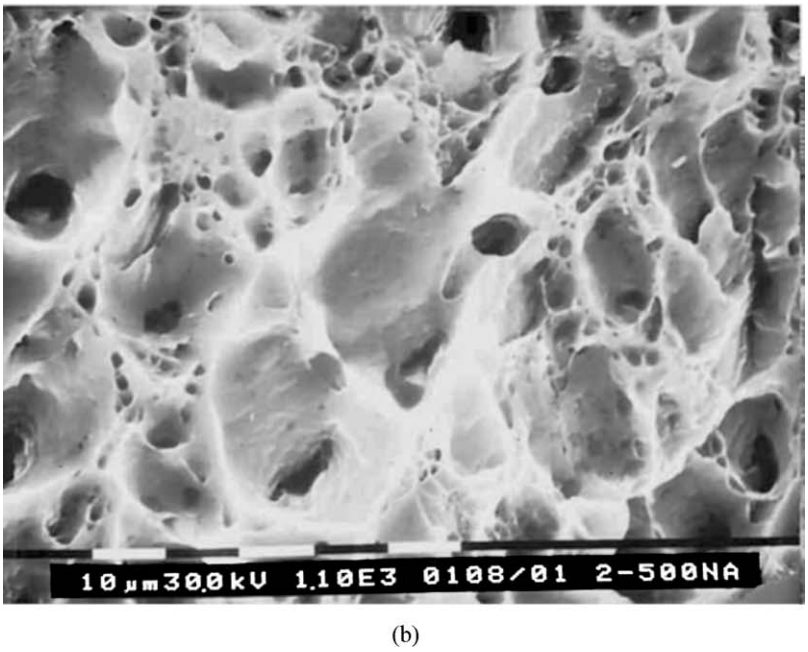

(b)

Figure 7 SEM fractograph of 2% prestrained AA6111 at: (a) 0 h and (b) 500 h natural aging.

possible that Mg-Si co-clusters may have formed [14, 15, 30]. The application of various levels of prestrain, it is believed, further increases the speed with which quenched in vacancies move to GPI zones and form at the high energy sites within the material with natural aging time.

In some other results of research underway, the dissolution reaction peak for quenched, unstrained and naturally aged samples have been observed to shift to higher temperatures with increasing natural aging time. This is attributed to a greater thermal stability of GPI zones resulting from their increased size. A close look at the dissolution peak B for the quenched, prestrained and naturally aged samples however, shows a shift to lower temperatures. The variation of DSC peak dissolution reaction temperature (T_P) of GPI zones with prestrain at room temperature for 24 h of natural aging times is plotted in Fig. 5 to illustrate this point. It can be observed that peak reaction temperature during GPI zone dissolution occurs at lower temperatures as the level of prestrain increases. This is attributed to sites of high energy generated in the material due to the increased dislocation density, causing the GPI zones to dissociate faster for the attainment of stability in the material during the DSC run.

3.3. Fractography

Figs 6–8 show the SEM fractographs of failed tensile specimens, which had been subjected to various levels of prestrain and naturally aged for up to 500 h. Fig. 6a and b show a comparison of the fractographs for the quenched unstrained samples and those subjected to 500 h natural aging. It can be observed from the two figures that there are more dimples on the 500 h naturally aged sample compared to the 0 h natural aging.

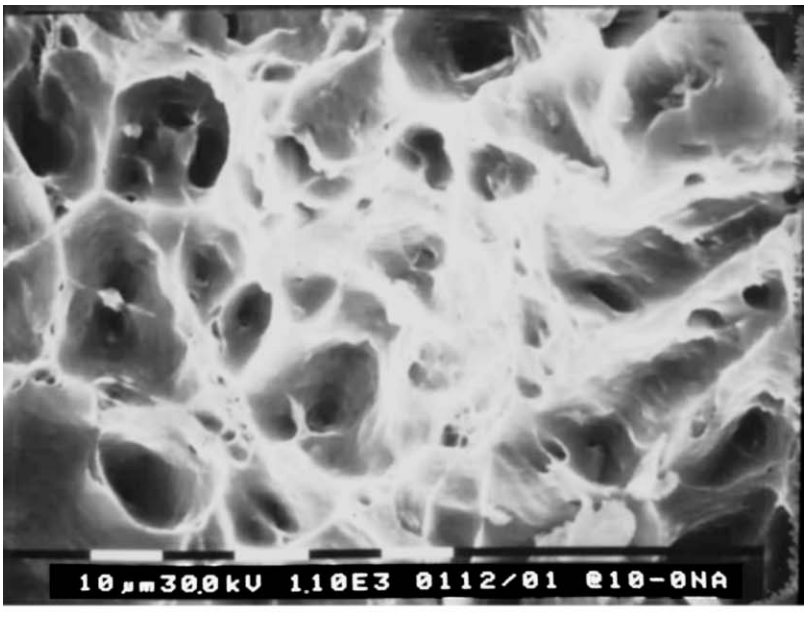

(a)

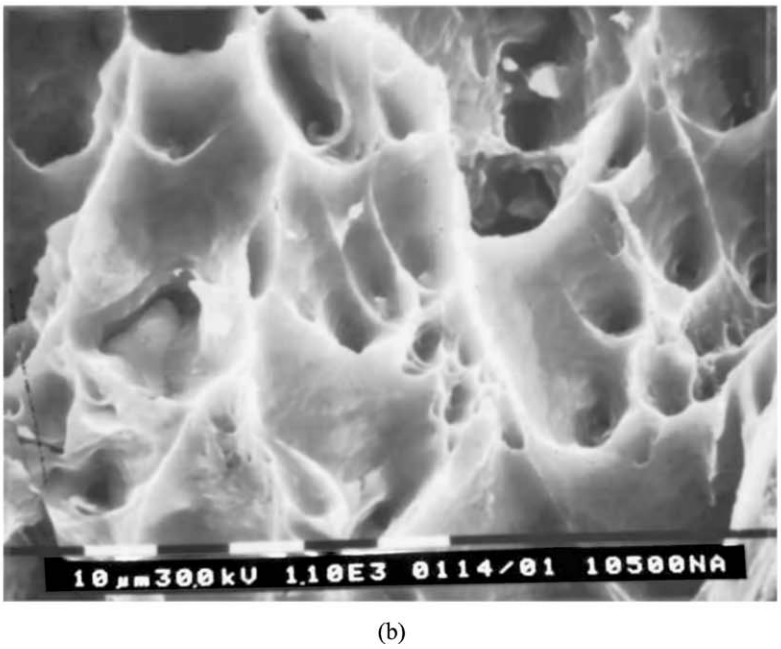

(b)

Figure 8 SEM fractograph of 10% prestrained AA6111 at: (a) 0 h and (b) 500 h natural aging.

This is attributed to clusters and stable GPI zones formed as a result of natural aging. Fig. 7a and b show a comparison of fractographs for quenched samples subjected to 2% prestrain with 0 and 500 h natural aging respectively. It can be observed that Fig. 5b has more dimples on its surface than in Fig. 7a. The formation of smaller dimples along the surface of the ledges between the bigger ones may be attributed to the interaction between dislocations and GPI zones, resulting in dislocations cutting GPI zone [31]. Furthermore, a comparison between Figs 6 and 7 show that the strained and naturally aged samples have more dimples on their surfaces than the unstrained samples. Thus, the application of prestrain prior to room temperature aging has a significant effect on the subsequent tensile ductility of these samples. Fig. 8a and b compare the fractographs of 10% prestrained samples subjected to 0 and 500 h natural aging respectively. A close look at these figures illustrates that some of the dimples are the result of the presence of second phase particles in the alloy. These particles have been identified, using EDS, to be intermetallics of the Al_xFeSi type [32]. They are believed to serve as initiation sites for fracture in the materials during tensile testing as the caps have been dislodged from the cones around them in addition to their dislodgement from GPI zones.

4. Conclusions

1. There is an increase in yield strength of 6111 aluminum with increasing levels of prestrain during natural aging, thus suggesting that dislocations interact with GPI zones to improve its strengthening characteristics under this condition.

2. The application of plastic prestrain does not alter the aging sequence of AA6111 significantly, as demonstrated by the tensile and DSC results. However, the speed with which the various phases form is enhanced.

3. The application of plastic prestrain changes the relative quantities of the various phases formed during natural aging, in particular, with a decrease in the volume fraction of GPI zones.

4. Prior prestrain and subsequent natural aging show improvement in the dimpled tensile fracture. However, the role of intermetallic particles is significant in that they serve as nucleation sites for fracture.

Acknowledgement

The authors would like to thank Dr. A. K. Gupta of Alcan International Limited, Kingston, Ontario for his technical contribution. Thanks are also due Dr. M. C. Chartevedi and his staff at the Metallurgy Laboratory, University of Manitoba, for allowing access to use their electron optics facilities. Government of Ghana Scholarship through the University of Cape Coast to G. K. Quainoo is gratefully acknowledged. Financial assistance from the Natural Sciences and Engineering Research Council of Canada (NSERC) in the form of a research grant to S. Yannacopoulos is hereby acknowledged.

References

1. M. H. MULAZIMOGLU, A. ZALUSKA, F. PARAY and J. E GRUZLESKI, *Metall. Mater. Trans.* A **28A** (1997) 1289.
2. D. W. PASHLEY, J. W. RHODES and A. SENDOREK, *J. Inst. Metals* **94** (1966) 41.
3. D. W. PASHLEY, M. H. JACOBS and J. T. VIETZ, *Phil. Mag.* **51** (1967) 16.
4. C. PANSERI and T. FEDERIGHI, *J. Inst. Metals* **94** (1966) 99.
5. S. CERSARA, E. DI RUSSO, P. FIORINI and A. GIARDA, *Mater. Sci. Engng.* **5** (1969/70) 220.
6. T. MOONS, P. RATCHEV, P. DESMET, B. VERLINDEN and P. VAN HOUTTE, *Scripta Mater.* **35** (1996) 939.
7. W. J. POOLE, D. J. LLOYD and J. D. EMBURY, *Mater. Sci. Engng.* A **234–236** (1997) 306.
8. M. TAMIZIFAR and G. W. LORIMER, Aluminum alloys: Their Physical and Mechanical Properties, in Proc. 3rd Int. Conf. Aluminum, edited by L. Arnberg, O. Lohne, E. Nes and N. Ryum (1992) Vol. 1, p. 220.
9. D. K. CHATTERJEE and K. M. ENTWISTLE, *J. Inst. Met.* **101** (1973) 53.
10. R. J. LIVAK, *Metall. Trans.* A **13A** (1982) 1318.
11. H. SUZUKI, M. KANNO and G. ITOH, *J. Jpn. Inst. Light Met.* **30** (1980) 606.
12. T. SAKURAI and T. ETO, Aluminum Alloys: Their Physical and Mechanical Properties, in Proc. 3rd Int. Conf. Aluminum, edited by L. Arnberg, O. Lohne, E. Nes and N. Ryum (Norwegian Institute of Technology and SINTEF Metallurgy, Trondheim, 1992) Vol. 1, p. 208.
13. D. J. CHAKRABARTI, B. K. CHEONG and D. E. LAUGHLIN, in "Automotive Alloys II," edited by S. K. Das (TMS, Warrendale, PA, 1998) p. 27.
14. M. MURAYAMA, K. HONO, M. SAGA and K. KIKUCHI, *Mater. Sci. Engng.* A **A250** (1998) 127.
15. M. MURAYAMA and K. HONO, *Acta Mater.* **47**(5) (1999) 1537.
16. G. BURGER, A. K. GUPTA, P. W. JEFFREY and D. J. LLOYD, *Mater. Char.* **33** (1995) 23.
17. A. K. GUPTA, P. H. MOROIS and D. J. LLOYD, in Proc. 5th Int. Conf. on Aluminum Alloys, Grenoble, France (Transtech, Zuerich-Uetikon, Switzerland, 1996) p. 801.
18. A. PEROVIC, D. D. PEROVIC, G. C. WEATHERLY and D. J. LLOYD, *Scripta Mater.* **41**(7) (1999) 703.
19. W. F. MIAO and D. E. LAUGHLIN, *Metall. Mater. Trans.* A **31A** (2000) 361.
20. *Idem., Scripta Mater.* **40**(7) (1999) 873.
21. K. M. ENTWISTLE, J. H. FELL and K. I. KOO, *J. Inst. Metals* **91** (1962/63) 84.
22. A. K. GUPTA and D. J. LLOYD, "Aluminum Alloys: Their Physical and Mechanical Properties," edited by L. Arnberg *et al.*, Norwegian Institute of Technology and SINTEF Metallurgy (Trondheim, 1992) Vol. 2, p. 21.
23. D. J. LLOYD, D. R. EVANS and A. K. GUPTA, *Canadian Metall. Quart.* **39**(4) (2000) 475.
24. E. C. FRANZ, *Light Metal Age* **43**(11/12) (1985) 12.
25. I. DUTTA and S. M. ALLEN, *J. Mater. Sci. Lett.* **10** (1991) 323.
26. C. BALDINI, F. MARINO and A. TOMASI, *Mater. Sci. & Engng.* **A 136**, 99.
27. J. M. PAPAZIAN, *Metall. Trans.* **19A** (1988) 2953.
28. P. BARCZY and F. TRANTA, *Scand. J. Metall.* **4** (1975) 284.
29. I. KOVACS, J. LENDVAI and E. NAGY, *Phys. Stat. Sol.* **14** (1972) 83.
30. G. A. EDWARDS, K. STILLER, G. L. DUNLOP and M. J. COUPER, *Acta Mater.* **46**(11) (1998) 3893.
31. D. M JIANG, B. D. HONG, T. C. LEI, D. A. DOWNHAM and G. W. LORIMER, *Mater. Sci. Techn.* **7** (1991) 1010.
32. G. K. QUAINOO, S. YANNACOPOULOS and A. K. GUPTA, *Canad. Metall. Quart.* **40**(2) (2001) 211.

Received 28 August 2003
and accepted 29 April 2004